

## Introduction of ISPG Method and Geometric Multiscale Modeling for Electronics Solder Reflow and Shock Wave Analysis

Dandan Lyu, Wei Hu, Xiaofei Pan, C. T. Wu

Computational and Multiscale Mechanics Group, Livermore Software Technology,  
An Ansys Company, Livermore, USA

### Abstract

Solder joints have become the main mechanical and electrical connections in modern microelectronics packaging for most consumer electronics products and they are typically observed to be the weakest links in terms for structural strength in the drop shock event. A drop shock simulation involves modeling the shock wave effect on mesoscale solder joints and macroscale chip packages concurrently, which is a typical multi-scale problem. Conventional finite element approaches using beam elements for the representation of the solders and the one-way sub-modeling technique cannot offer a high-fidelity solution. In addition, the shape of the solder ball is a very important contributory factor in determining the local stress levels and it is impractical to obtain all solder ball geometries by experimental measurement. Therefore, an effective simulation tool for the prediction of solder ball shape in the solder joint design as well as for the drop shock analysis is required in electronics industry.

In this paper, a multiscale computational approach for linking the information of mesoscale dissimilar solder ball geometries to the macroscale drop shock of a printed circuit board (PCB) <sup>[1]</sup> is developed. To begin, an implicit incompressible smoothed particle Galerkin (ISPG) <sup>[2]</sup> method is introduced to model the free-surface solder reflow process and predict the solder ball shapes. The formulation considers the surface tension of molten solder and the wall adhesion between the solder and the substrate. Subsequently, the predicted solder ball shapes from the reflow analysis are used in a chip package model for the drop shock analysis. The mesoscale solder joint model is coupled concurrently with the macroscale chip package model using an explicit-explicit non-intrusive two-scale coupling method via the co-simulation technique. An algorithm that handles properly the load-balancing, heterogeneity of processors and memory also has been developed to achieve the practical non-intrusive scale-bridging effect.

Numerical examples firstly demonstrate that the proposed implicit ISPG formation is able to accurately and efficiently predict the solder reflow profile. Then a multiscale drop shock example utilizing the reflowed solder ball shapes for a chip-scale package is performed, which indicates that the present approach is capable of delivering an accurate and efficient solution by comparing to the (direct numerical simulation) DNS results.

### 1 Introduction

Solder joints are critical part for mechanical and electrical connections in modern microelectronics packaging of electronics. Due to the toxicity of lead (Pb), modern solder materials are often required to be lead free. Such lead-free solders are more brittle in nature and easily susceptible to failure, thus they are regarded as the weakest points in printed circuit board (PCB)<sup>[3]</sup>, which results in a higher risk of solder joints failures. If one solder joint fails in a PCB, the whole electronic system may break down. Therefore, the drop shock reliability and failure analysis of lead-free solder joints has become critical in the electronic product design and engineering. During the product's virtual development process, extensive computer simulations of drop test are conducted using commercial explicit finite element codes such as LS-DYNA and ABAQUS to study the drop shock response of the solder joints before the designed printed circuit board (PCB) and electronic assembly are ready for production.

A drop shock simulation involves modeling the shock wave effect on mesoscale solder joints and macroscale chip packages concurrently, which is a typical multi-scale problem. Conventional finite element approaches using beam elements for the representation of the solders and the one-way sub-modeling technique cannot offer a high-fidelity solution. In addition, the shape of the solder ball is a very important contributory factor in determining the local stress levels and it is impractical to obtain all solder ball geometries by experimental measurement. Therefore, an effective simulation tool for the prediction of solder ball shape in the solder joint design as well as for the drop shock analysis is required in electronics industry.

The goal of the present study is to develop a new computational approach via a co-simulation technique to provide insights for chip scale drop tests. An effective analysis of solder joints in drop shock event requires an accurate solder ball reflow simulation for the prediction of mesoscale solder ball geometry as well as a meso-macroscale coupling method for the explicit dynamics analysis. The remainder of the paper is arranged as follows: an overview of a full-implicit incompressible smoothed particle Galerkin (ISPG) method is introduced in Section 2 to model the solder reflow process and predict the solder ball shape. The formulation considers the surface tension of molten solder and the wall adhesion between the solder and the substrate. Section 3 describes the explicit-explicit non-intrusive two-scale coupling method and its weak formulation for the drop test simulation. LS-Dyna keywords about ISPG approach and two-scale Co-simulation are given in Section 4. Numerical examples are given in Section 5, and conclusions are made in Section 6.

## 2 Implicit ISPG Formulation for Solder Reflow

### 2.1 Governing Equations

The lead-free solder reflows at a fixed temperature near the solder melting (eutectic) point. Therefore, the solder reflow process inside the reflow oven is usually considered in an isothermal state. In numerical simulation, this fluid-like solder reflow behavior is described by the Navier-Stokes equation. In this paper, the Lagrangian Navier-Stokes equation is used to describe the free surface reflow process where the governing equation comprising the pressure term, the viscosity term and the gravity term can be written as

$$\frac{D\mathbf{v}}{Dt} = -\frac{1}{\rho}\nabla p + \frac{\vartheta}{\rho}\nabla^2\mathbf{v} + \mathbf{g} \quad (1)$$

where  $\mathbf{v}$ ,  $\rho$ ,  $p$  are fluid velocity, density, and pressure, respectively.  $\vartheta$  is the dynamic viscosity,  $t$  denotes the time, and  $\mathbf{g}$  is the gravity. The incompressible condition is enforced using the continuity equation in a standard way and is given by:

$$\nabla \cdot \mathbf{v} = 0 \quad (2)$$

It is well-understood that numerical instability arises in the numerical simulation of incompressible flows when the velocity and the pressure are coupled by the incompressibility constraint. To overcome this numerical issue, the 2nd order generalized rotational incremental pressure-correction (GRIPC) scheme (Guermond et al., 2006) is implemented as a fractional step method for the reflow study. In the first sub step of the 2nd order GRIPC scheme, we have

$$\frac{1}{\Delta t}(\mathbf{v}^{n+1*} - \mathbf{v}^n) = -\frac{1}{\rho}\nabla p^n + \frac{\vartheta}{\rho}\nabla^2\mathbf{v}^{n+1*} + \mathbf{g}, \mathbf{v}^{n+1*}|_{\Gamma_v} = \bar{\mathbf{v}} \quad (3)$$

In the second sub step of the 2nd order GRIPC scheme, the velocities are corrected through the following equation

$$\frac{1}{\Delta t}(\mathbf{v}^{n+1} - \mathbf{v}^{n+1*}) + \frac{1}{\rho}\nabla\phi^{n+1} = 0, \mathbf{v}^{n+1}|_{\Gamma_v} = \bar{\mathbf{v}} \quad (4)$$

where the variable  $\phi$  is defined as

$$\phi^{n+1} = p^{n+1} - p^n + \vartheta\nabla \cdot \mathbf{v}^{n+1*} \quad (5)$$

The corrected velocity in Eq. (4) must satisfy the divergence-free condition, which yields the following Poisson equation,

$$\nabla \cdot \mathbf{v}^{n+1*} = \frac{\Delta t}{\rho}\nabla^2\phi^{n+1} \quad (6)$$

From Eq. (4), it's observed that the Neumann boundary condition  $\nabla\phi^{n+1} \cdot \mathbf{n}|_{\Gamma_v} = 0$ . The Dirichlet boundary condition at the free surface can be induced from Eq. (5), that is

$$(\phi^{n+1} + p^n - \vartheta\nabla \cdot \mathbf{v}^{n+1*})|_{\Gamma_p} = p^{fs} \quad (7)$$

where  $\Gamma_p$  is the free surface boundary, and  $p^{fs}$  is the pressure at the free surfaces.

### 2.2 Surface Tension

During the reflow process, the surface tension causes a pressure jump  $\sigma_\kappa^{fs}$  at the interface between the liquid solder and air proportional to the mean curvature of the interface

$$\sigma_\kappa^{fs} = \gamma\kappa \quad (8)$$

where  $\gamma$  is the surface tension coefficient, and  $\kappa = -\nabla \cdot \mathbf{n}$  is the mean curvature, and  $\mathbf{n}$  is the inward norm direction of the liquid solder surface. Subsequently, the pressure term applied at the essential pressure boundary condition can be calculated as

$$p^{fs} = p^{air} + \sigma_{\kappa}^{fs} \quad (9)$$

The surface tension will work against the earth's gravity during the solder reflow process.

### 2.3 Surface Tension

When molten solder is in contact with the substrate, the solder liquid interface forms a contact angle  $\theta$  with the wall boundary. If the angle  $\theta$  is equal to static contact angle  $\theta_{eq}$ , a state of static equilibrium is reached. If not, then a nonzero wall adhesion force tends to pull the interface to the equilibrium position. In our algorithm, the wall adhesion boundary condition can be expressed by the unit free surface normal  $\mathbf{n}$  at the interface point  $\mathbf{x}_w$  shown in Fig. 1.

$$\mathbf{n}(\mathbf{x}_w) = \mathbf{n}_w \cos(\theta_{eq}) + \mathbf{t}_w \sin(\theta_{eq}) \quad (10)$$

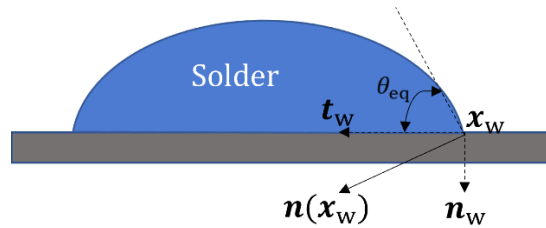


Figure 1: Illustration of the wall adhesion

Using the 2nd generalized rotational incremental pressure-correction scheme, the weak form of incompressible flow problem can be formulated within the Galerkin framework using the Lagrangian approach and the particle approximation, the details of the formulation can be found in reference [2].

## 3 Two-scale Co-simulation for Shock Wave Analysis

A two-scale coupling approach that incorporates the reflowed solder joints with the chip package using the co-simulation for an efficient drop test simulation is described in this section. This type of concurrent multiscale methods<sup>[4]</sup> is called as the non-intrusive approach where data exchanges between mesoscale solder joints and the macroscale chip package concern only nodal forces and velocities in the interface zone. Different from the classical two-scale coupling method, co-simulation<sup>[5]</sup> often refers to a numerical approach coupling different subsystems of a model and simulating them in a distributed manner. It combines two or more separate analyses using same or different simulation codes and runs at different time scales. Recently, co-simulation also has been combined with the domain decomposition technique to solve the multiscale problems using the explicit-explicit coupling in transient dynamic analysis. Several global-local methods employing different data exchanges<sup>[6][7]</sup> have been developed to substantially reduce the computational cost of explicit dynamic analysis in co-simulation.

### 3.1 Weak Formulation of the Two-Scale Coupling System

In a two-scale coupling system, the variational equations for a transient dynamic problem can be formulated using the integration by part to find the macroscale (global) displacement field  $\mathbf{u}^G(\mathbf{X}^G, t) \in V^G = \{\mathbf{u}^G \in H^1(\Omega^G): \mathbf{u}^G = \mathbf{u}_g \text{ on } \partial\Omega_g\}$  and the mesoscale (local) displacement field  $\mathbf{u}^L(\mathbf{X}^L, t) \in V^L = \{\mathbf{u}^L \in H^1(\Omega^L): \mathbf{u}^L = \mathbf{u}^G \text{ on } \partial\Omega_c\}$ , such that for arbitrary variation  $\delta\mathbf{u}^G \in V_0^G = \{\mathbf{u}^G \in H^1(\Omega^G): \mathbf{u}^G = 0 \text{ on } \partial\Omega_g\}$  and  $\delta\mathbf{u}^L \in V_0^L = \{\mathbf{u}^L \in H^1(\Omega^L): \mathbf{u}^L = 0 \text{ on } \partial\Omega_c\}$ , the following equations are satisfied:

$$\int_{\Omega^G} \rho \ddot{\mathbf{u}}^G \cdot \delta\mathbf{u}^G d\Omega + \int_{\Omega^G} \boldsymbol{\sigma} : \nabla^s(\delta\mathbf{u}^G) d\Omega = \int_{\Omega^G} \mathbf{b} \cdot \delta\mathbf{u}^G d\Omega + \int_{\partial\Omega_n} \mathbf{h} \cdot \delta\mathbf{u}^G ds + \int_{\partial\Omega_c} \mathbf{f}^c \cdot \delta\mathbf{u}^G ds \quad (11)$$

$$\int_{\Omega^L} \rho \ddot{\mathbf{u}}^L \cdot \delta\mathbf{u}^L d\Omega + \int_{\Omega^L} \boldsymbol{\sigma} : \nabla^s(\delta\mathbf{u}^L) d\Omega = 0 \quad (12)$$

where  $\Omega^G$  and  $\Omega^L$  denote the macroscale and mesoscale domains, respectively.  $\mathbf{b}$  is the body force vector and  $\boldsymbol{\sigma}$  is the Cauchy stress obtained from the constitutive law. The  $\partial\Omega_g$  notation describes a Dirichlet boundary imposed by a displacement  $\mathbf{u}_g$  and  $\partial\Omega_n$  is the Neumann boundary prescribed by a surface traction  $\mathbf{h}$  with  $\partial\Omega_g \cap \partial\Omega_n = 0$ .  $\partial\Omega_c$  is the coupling interface of two scales as shown in Fig. 2, where the kinematic constraint equations  $\mathbf{u}^L = \mathbf{u}^G, \dot{\mathbf{u}}^L = \dot{\mathbf{u}}^G$  are imposed in the mesoscale computation and  $\mathbf{f}^c$  is the constrained force computed from the mesoscale.

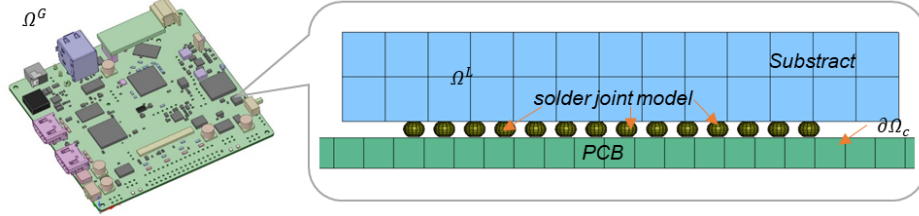


Figure 2: Two-scale models of solder joints in large scale structure

By substituting the FEM approximations  $\mathbf{u}^G(\mathbf{X}^G, t) = \sum_l N_l^G(\mathbf{X}^G) \mathbf{U}_l^G(t)$ ,  $\mathbf{u}^L(\mathbf{X}^L, t) = \sum_l N_l^L(\mathbf{X}^L) \mathbf{U}_l^L(t)$  into Eqs. (11) and (12), the semi-discrete equations can be expressed by the following algebraic equations

$$\mathbf{M}^G \ddot{\mathbf{U}}^G = \mathbf{F}^{ext} + \mathbf{F}^c - \mathbf{F}_{int}^G \quad (13)$$

$$\mathbf{M}^L \ddot{\mathbf{U}}^L = -\mathbf{F}_{int}^L \quad (14)$$

where

$$\mathbf{M}_{IJ}^G = \int_{\Omega^G} \rho N_I^G N_J^G Id\Omega \quad (15)$$

$$\mathbf{F}_I^{ext} = \int_{\Omega^G} \mathbf{b} N_I^G J_0 d\Omega + \int_{\partial\Omega_n} \mathbf{h} N_I^G ds \quad (16)$$

$$\mathbf{F}_I^c = \int_{\partial\Omega_c} \mathbf{f}_I^c ds \quad (17)$$

$$\mathbf{F}_{int,I}^G = \int_{\Omega^G} \boldsymbol{\sigma}_0 : \nabla_{\mathbf{X}^G} N_I^G d\Omega \quad (18)$$

$$\mathbf{M}_{IJ}^L = \int_{\Omega^L} \rho N_I^L N_J^L Id\Omega \quad (19)$$

$$\mathbf{F}_{int,I}^L = \int_{\Omega^L} \boldsymbol{\sigma}_0 : \nabla_{\mathbf{X}^L} N_I^L d\Omega \quad (20)$$

where  $N^G$  and  $N^L$  are approximation functions in the macro and meso scales, respectively.  $\boldsymbol{\sigma}_0$  is the first Piola-Kirchhoff stress tensor.

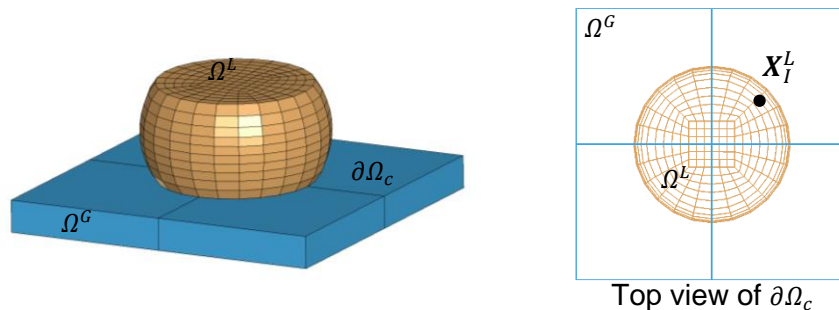


Figure 3: The non-conforming coupling interface between macroscale and mesoscale mesh

Considering the non-conforming mesh shown in Fig. 3 at the interface across two scales, the kinematic constraints in the mesoscale are approximated as follows:

$$\mathbf{U}_I^L \equiv \mathbf{U}^L(\mathbf{X}_I^L) = \sum_J N_J^G(\mathbf{X}_I^L) \mathbf{U}_J^G, \text{ for } \forall \mathbf{X}_I^L \in \partial\Omega_c \quad (21)$$

$$\dot{\mathbf{U}}_I^L \equiv \dot{\mathbf{U}}^L(\mathbf{X}_I^L) = \sum_J N_J^G(\mathbf{X}_I^L) \dot{\mathbf{U}}_J^G, \text{ for } \forall \mathbf{X}_I^L \in \partial\Omega_c \quad (22)$$

The constrained force can be computed by integrating all the contribution from the mesoscale internal force at the coupling interface  $\partial\Omega_c$  as follows:

$$\mathbf{F}_I^c \equiv \mathbf{F}^c(\mathbf{X}_I^c) = \sum_J N_I^G(\mathbf{X}_I^c) \mathbf{F}_{int,J}^L, \text{ for } \forall \mathbf{X}_I^c \in \partial\Omega_c \quad (23)$$

#### 4 LS-DYNA Keyword of ISPG and Two-scale Co-simulation

##### 4.1 LS-DYNA Keyword of ISPG

ISPG has been implemented in LS-DYNA as a new 3D element formulation (#49) in the keyword \*SECTION\_FPD for the fully implicit dynamic analysis. The ISPG nodes are automatically converted from those of the user's FEM model.

The input deck of \*SECTION\_FPD for card 2 and card 3 is described as follows:

Card 2	DX	DY	DZ	ISPLINE	KERNEL	BOX	SMSTEP	SSTYPE
	1.6	1.6	1.6	0	0			
Card 3				TSTART	DT_IMPL		DTSCCL_ISPG	

- DX,DY,DZ Normalized dilation parameters of the kernel function in X, Y and Z directions, the recommended range in ISPG is 1.4~1.8
- KERNEL Kernel type. KERNEL=0 Updated Lagrangian (UL) kernel. Currently, only UL kernel is supported.
- TSTART Starting time for the fully implicit ISPG iteration. Before TSTART, only 10 ISPG iterations are done in each structural implicit step to guarantee the fluid moves with the solid boundaries. After TSTART, the ISPG will do a full iteration in the structural implicit step. This option is very useful for cases where the structural simulation time is very long (e.g. in seconds or minutes), while the reflow process to a steady state is very short. With this option, we can let the full ISPG iteration start from TSTART and save some computational resources.
- DT\_IMPL Reset the implicit structural time step size to DT\_IMPL after TSTART. Because the solder reflow process is very fast, a small implicit structural time step size is needed. Generally, the value of DT\_IMPL should be around 10~50 times of ISPG time step size to guarantee the convergence of the solution if the gravity-driven simulation is deployed.
- DTSCCL\_ISPG The time step size scaling factor for ISPG iteration. 0.1~0.5 is recommended. Large DTSCALE\_ISPG may cause contact detection issues.

The material property of the fluid in ISPG is defined with the keyword \*MAT\_IFPD, the card 1 is described as follows:

Card 1	MID	RO	DYNVIS	SURFTEN				
	1							

- RO Fluid density
- DYNVIS Dynamic viscosity of the fluid
- SURFTEN Surface tension coefficient

The contact between fluid and solid is defined with the keyword \*DEFINE\_FP\_TO\_SURFACE\_COUPLING, the cards 1 and 2 are described as follows:

Card 1	SLAVE	MASTER	STYPE	MTYPE				
	1	1	1	0				
Card 2	SBC	SCA				SFP		
	0	0.5				0.1		

SLAVE Slave part/part set ID  
 MASTER Master segment set ID  
 STYPE Slave type, STYPE=1, slave part; STYPE=0, slave part set  
 MTYPE Master type, MTYPE = 0, segment set  
 SBC Type of boundary condition. SBC=0, free-slip boundary; SBC=1, non-slip boundary  
 SCA Static (equilibrium) contact angle  
 SFP Stiffness coefficient along the normal direction of the contact interface (SFP<1.0)

#### 4.2 LS-DYNA Keyword of Two-scale Co-simulation

To define coupling interface across two models in different scales running on MPI based co-simulation, keyword \*INCLUDE\_COSIM is implemented. The input deck format of \*INCLUDE\_COSIM is described as follows:

Card 1	1	2	3	4	5	6	7	8
	FILENAME							

FILENAME Name of an input file that contains the coupling information, which includes sets of segments in global scale model and sets of nodes in local scale one.

This keyword defines the coupling interface to exchange kinematic and kinetic information between global (large-scale) and local (small-scale) models running on two LS-DYNA MPP jobs. In real application, the global model is usually large-scale structure, e.g. full car model or printed circuit board (PCB), while the local model, e.g. spotwelds, rivets and solders, is relatively much smaller in dimension that leads to smaller mesh and time step size in explicit analysis. To accelerate the computation across global and local scales, users are able to use two input files and run two LS-DYNA MPP jobs simultaneously with different time step sizes. The synchronization of time stepping information across coupling interface is performed automatically at every time step of global model, while the time step size of local model is adjusted accordingly to guarantee the numerical consistency and accuracy of state variables at the coupling interface in spatial and temporal domain.

The coupling interface consists of two sets of entities: One set of segments using \*SET\_SEGMENT is defined for the global model at the coupling interface, and included in the global input deck using \*INCLUDE\_COSIM; The other set of nodes using \*SET\_NODE is defined for the local model at the coupling interface, and included in the local input deck using \*INCLUDE\_COSIM. These two sets defined in global and local included files must have the same set ID (SID) to enable the coupling between global and local jobs. Multiple sets of segments and nodes can be defined in the included files using \*INCLUDE\_COSIM for different coupling interfaces.

Two types of coupling algorithms are currently implemented: (a) Tied contact, where the set of segments in global model drives the motion of the set of nodes in local model by imposing the kinematic constraints on nodal translational DOFs, and the local model returns the constraint forces interpolated onto the nodes of the set of global segments. In this case, it must specify the flag 'ITS' as 1 in both \*SET\_SEGMENT and \*SET\_NODE. (b) Solid-in-shell immerse, where the local solid model occupies the same space as global shell model at the coupling interface. The set of nodes in local model follows both the translational and rotational motion of the set of shell segments in global model, while the nodes of the global segments obtain the constraint forces and moments as return. In this case, it must specify the flag 'ITS' as 2 in both \*SET\_SEGMENT and \*SET\_NODE. For the details and examples of how to run co-simulation jobs, please refer to the latest version of LS-DYNA manual [8].

## 5 Numerical Examples

### 5.1 ISPG for Solder Ball Shape Prediction

The implicit ISPG formation is shown to be able to predict the solder reflow profile accurately and efficiently in previous work [1]. In this example, we will investigate the assembly of PCB board with various chip packages and solder joints. The assembly consists of 72 solder joints shown in Fig. 4. The original geometries of the solder joints are modelled as cylinders with diameter of 1.2mm and height of 0.8mm. The solder will be deformed under the surface tension and the gravity of chip packages. The assembly is first uniformly heated from 438K to the reflow temperature of 538K. The boundary conditions on the chip packages are then released, so that it can displace under gravity until the total reaction force from all solders balances its weight. The solder material considered for this simulation is 63Sn-37Pb. Its density is  $8.9\text{g/cm}^3$ , the dynamic viscosity is  $2.24\text{E-}03\text{Pa}\cdot\text{s}$  and surface tension is  $49.85\text{N/m}$  [9].

The finite element mesh for the model has 53634 nodes and 95358 elements. The deformed shape of the package assembly is shown in Fig. 5. Different solder joint geometries can be observed, which is caused by different weight of the chips and the different position connecting with the chips. The variation in solder shapes of the top and bottom chips are demonstrated in Fig. 6 (a) and (b), respectively.

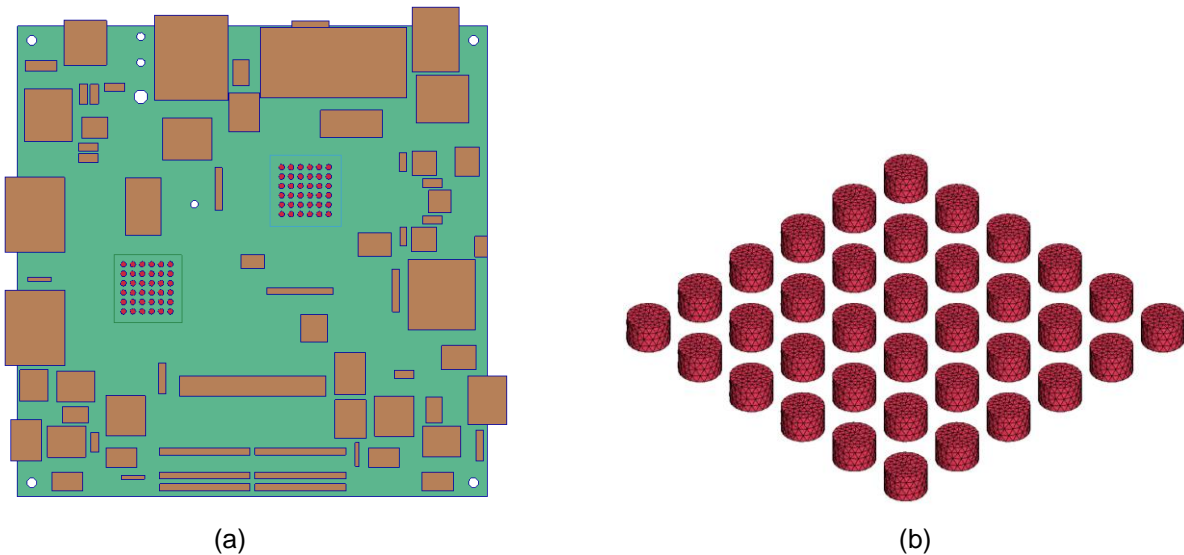


Figure 4(a): The setup of PCB with various chip packages and solder joints; (b) Mesh of solder joints connected with the top chip

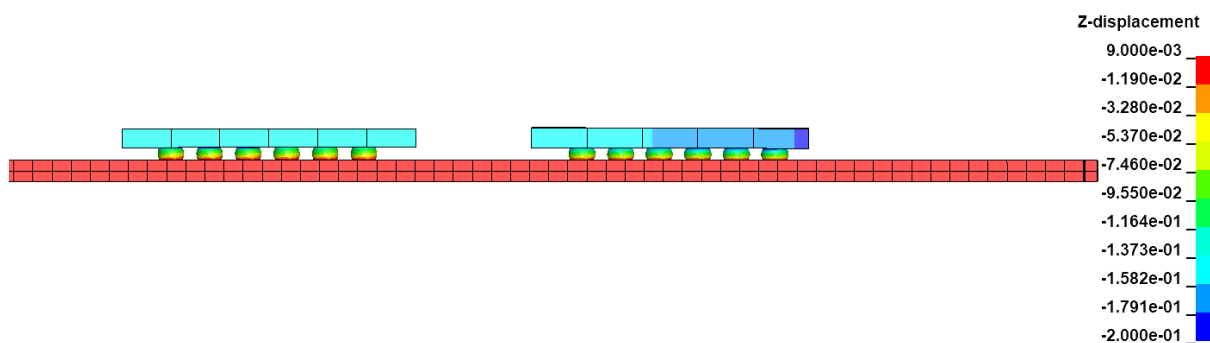


Figure 5: Final deformation of the PCB assembly (z displacement contour: mm)

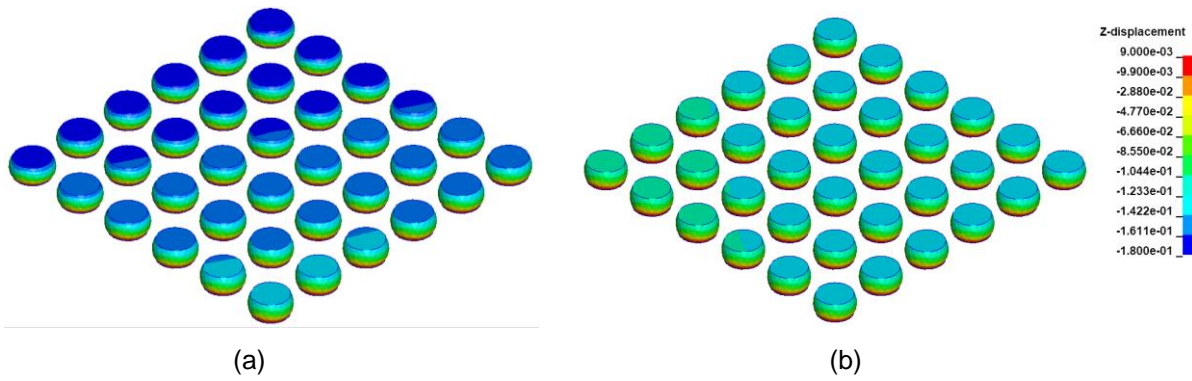


Figure 6: Final configuration of the deformed solders connected with (a) top chip (b) bottom chip (z displacement contour: mm)

## 5.2 Shock Wave Analysis of Printed Circuit Boards

Using the deformed shape of solder in the previous section, this PCB assembly is dropped to a rigid base plate and shock wave analysis was performed. The material property of solders is identical to that in reflow analysis. The analyses of macroscale model and mesoscale model are performed in two separated simulation jobs with information exchange using the framework shown in Fig. 7.

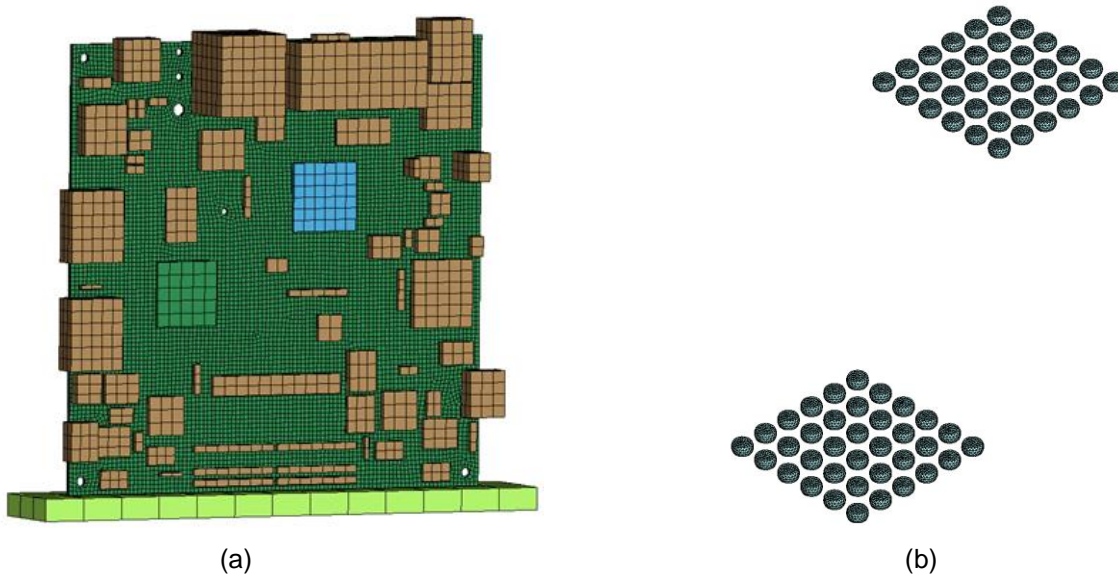


Figure 7: Finite element mesh of macroscale and mesoscale model: (a) macroscale model; (b) mesoscale model.

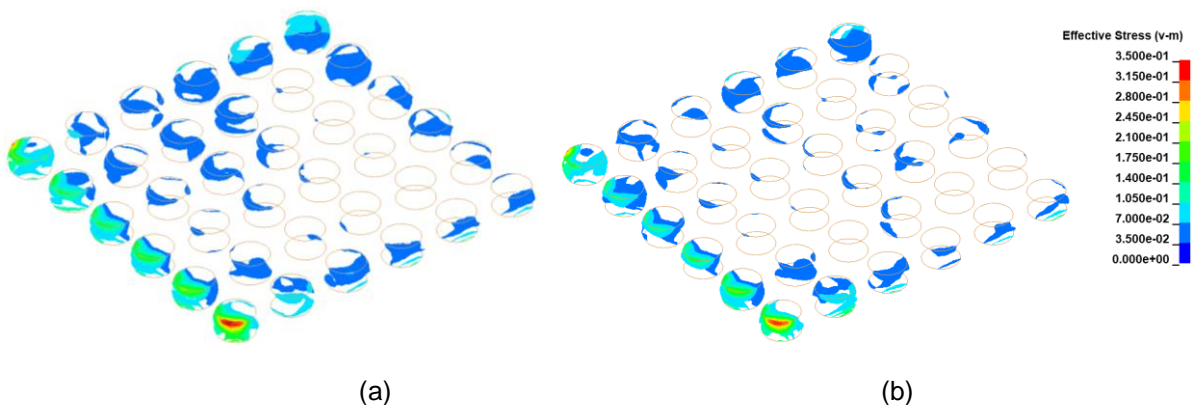


Figure 8: Von Mises stress distribution at the bottom interface of solder balls: (a) Two-scale co-simulation (GPa); (b) DNS (GPa)

The predicted distribution of von Mises stress in the solder balls by two-scale co-simulation and DNS is compared in Fig. 8. Both the distribution and the magnitude of von Mises stress match very well. It shows that the corner solder ball at the top chip has the largest von Mises stress and is the most critical solder ball.

The displacement evolution at the solder interface by two-scale co-simulation and DNS is compared in Fig. 9. (a). The evolution of von Mises stress at one of elements in the most critical solder ball is also compared in Fig. 9 (b). Excepting local oscillations, the results using two-scale so-simulation match well with DNS.

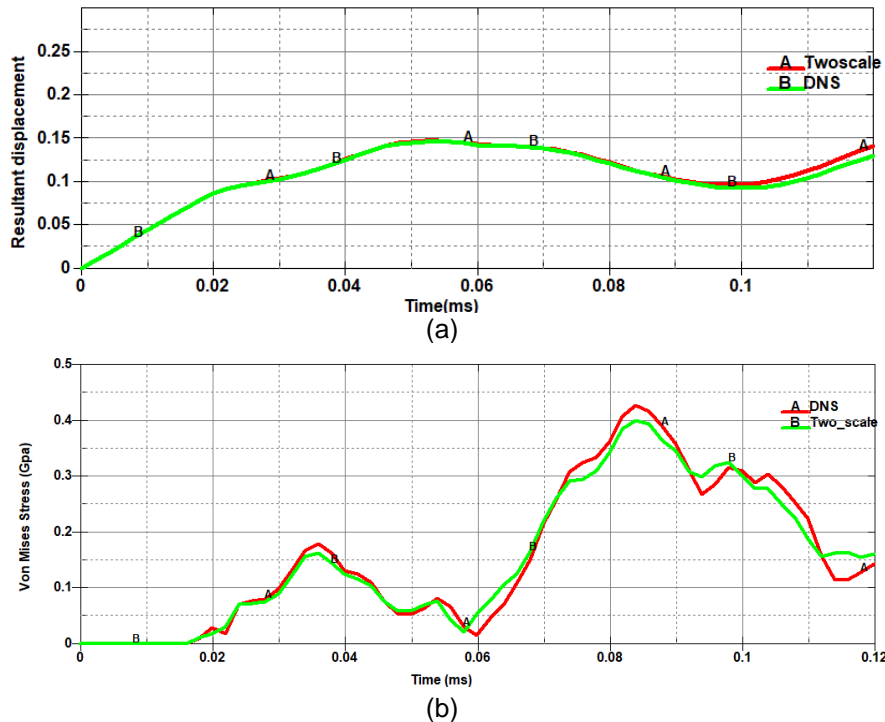


Figure 9: Comparison of displacement and Von Mises stress evolution (a) resultant displacement of the most critical solder joint interface (b) Von Mises stress of the most critical solder ball

In terms of computational cost, two-scale co-simulation costs around 9 minutes with 4 CPU cores (1 for macroscale model and 3 for mesoscale model), while DNS takes around 33 minutes using the same number of CPU cores. The normalized computation time comparison ratio is around 0.27. A high efficiency can be achieved by two-scale co-simulation system with great accuracy.

## 6 Summary

In this paper, an implicit ISPG formulation incorporating the surface tension and cohesion force terms is developed for simulating the free-surface solder reflow process. This new method allows engineers to efficiently establish the geometry of solder joint in the mesoscale level prior to performing solder joint reliability analysis in the macroscale. Second, an explicit-explicit non-intrusive two-scale coupling method via the co-simulation technique is introduced to the two-scale system for the drop test simulation. This multiscale approach permits a new two-way coupling between the mesoscale solder joint model and macroscale chip package model for the drop shock analysis. The present approach avoids a tedious matching mesh issue and compromises the accuracy and efficiency requirements in the industrial application. The two numerical examples in this paper present a new multiscale simulation utilizing the reflowed solder ball shapes for the drop test of a chip-scale package. In comparison to the DNS result, the multiscale result indicates that the present method can deliver an accurate and efficient solution.

## 7 Literature

- [1] Hu, W., Pan X., Lyu D., Srivastava A., Shah S., Wu, C.T.: "A Two-scale approach for the drop shock simulation for a printed circuit board package considering reflowed solder ball geometries", *International Journal for Multiscale Computational Engineering*, 18(4), 2020, 455-476.
- [2] Pan, X., Wu, C. T. and Hu, W.: "A semi-implicit stabilized particle Galerkin method for incompressible free surface simulations", *International Journal for Numerical Methods in Engineering*, 121(17), 2020, 3979-4002.
- [3] Chong, D. Y. R., Che, F. X., Pang, J. H. L., Ng, K., Tan, J. Y. N. and Low, P. T. H.: "Drop impact reliability testing for lead-free and lead-based soldered IC packages", *Microelectronics Reliability*, 46, 2006, 1160-1171.
- [4] Gendre, L., Allix, O., Gosselet, P. and Comte, F.: "Non-intrusive and exact global/local techniques for structural problems with local plasticity", *Computational Mechanics*, 44, 2009, 233-245.
- [5] Dehning, C., Bierwisch, C. and Kraft, T.: "Co-simulations of Discrete and Finite Element Codes. In: Griebel, M., Schweitzer, M. (eds) *Meshfree Methods for Partial Differential Equations VII.* ", *Lecture Notes in Computational Science and Engineering*, 100, Springer, Cham, 2015.
- [6] Bettinotti, O., Allix, O., Perego, U., Oancea, V. and Malherbe, B.: "Simulation of delamination under impact using a global-local method in explicit dynamics", *Finite Elements in Analysis and Design*, 125, 2017.1-13
- [7] Ahmed N. and Xue, P.: "Determination of the size of the local region for efficient global/local modeling in a large composite structure under impact loading", *International Journal of Impact Engineering*, 144, 2020, 103646.
- [8] Hallquist JO (2019) *LS-DYNA Keyword User's Manual*, Livermore Software Technology, an ANSYS company, Livermore, California
- [9] Chou, Y.-Y., Chang, H.-J., Kuo, J.-H., & Hwang, W.-S.: "The Simulation of Shape Evolution of Solder Joints during Reflow Process and Its Experimental Validation", *Materials Transactions*, 7(4), 2006, 1186–1192.